DOI: 10.1002/anie.200906891

Photoactive Devices

Innovative Inorganic–Organic Nanohybrid Materials: Coupling Quantum Dots to Carbon Nanotubes**

*Christian Schulz-Drost, Vito Sgobba, Christina Gerhards, Susanne Leubner, Rafael M. Krick Calderon, Andrés Ruland, and Dirk M. Guldi**

Nanoscale systems are presaged to be a competitive means of transforming molecular and bulk electronic structures into easily processible, but intricate materials.[1] In this context, semiconductor nanoparticles and carbon nanostructures serve as ideal building blocks for the design of optoelectronic devices.[2–5] Owing to the outstanding features of CdTe quantum dots (QDs), namely sizeable absorptions throughout the UV and near-IR spectral regions,[6] narrow and widely tunable photoluminescence,[7] and high photostability,[8] their close resemblance to bulk inorganic semiconductors has motivated intense studies and has led to the realization of numerous applications.[9]

Future scientific and technological breakthroughs will depend, in large, on key achievements such as electronically coupling these crystalline QDs to other functional materials. The unique structure and composition of single-walled carbon nanotubes (SWNTs), that is, their extended, delocalized π-electron system and wide range of distinctive properties, renders them ideal for the fabrication of lightweight, inexpensive, and flexible electronics once they are linked to suitable electron donors.[10] To this end, we recently documented a milestone in the solubilization of SWNTs in aqueous media by means of immobilization of charged pyrene derivatives. Subsequent association of CdTe QDs through electrostatic interactions afforded nanohybrids, which were successfully integrated into multifunctional layer-by-layer (LbL) nanoconstructs that featured appreciable photocurrent performances.[10a] Despite their simplicity and effectiveness, the use of equilibria driven by π–π stacking and/or electrostatic attractions is not generally applicable because of the lack of long-term stability, high sensitivity to changes in pH and ionic strength, and difficult control of stoichiometry and morphology.

We report herein on a novel strategy en route to QD/SWNT nanohybrids, namely the covalent attachment of pyrene to CdTe QDs to afford QD-pyrene nanoconjugates; these bind to the surface of SWNTs through π–π stacking interactions between pyrene and the SWNT to yield QD-pyrene/SWNT nanohybrids (Scheme 1). The systematic preparation and characterization of both the individual building blocks and the nanohybrid in solution will be ultimately beneficial for the understanding of electronic interactions in solution-processed solar cells.

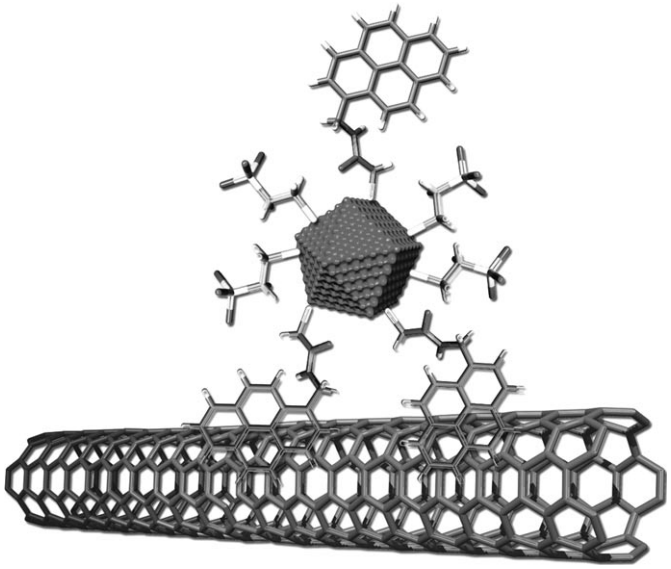

Scheme 1. QD-pyrene/SWNT nanohybrid.

The CdTe QDs were prepared by modifying a previously reported method.[11] In the current work, thioglycolic acid (TGA) and 2-mercaptoethanesulfonate (MESNA) were chosen to co-stabilize QDs through binding of their thiol groups; the hydrophilic groups (i.e., carboxylic acids and sulfonates) are exposed to the solvent. MESNA ensures exclusively the solubility in water, whereas TGA enables the covalent attachment of 1-pyrenemethylamine through peptide condensation. All crude QD samples were purified by precipitation upon addition of ethanol. For optical and microscopic characterization and/or association with SWNT, the dry powder was redissolved in Millipore water or aqueous 2-(*N*-morpholino)ethanesulfonic acid (MES), respectively.

The QDs were covalently bound to 1-pyrenemethylamine by EDC/NHS-mediated peptide condensation to form QD-pyrene nanoconjugates (EDC = 1-ethyl-3-(3-dimethylaminopropyl)carbodiimide, NHS = *N*-hydroxysuccinimide). Amide bond formation was corroborated by IR spectroscopy (Figure S1 in the Supporting Information). The QDs display distinct IR absorption features in the region between 3650 and 3000 cm^{-1} (ν(OH), H_2O), at 1570 cm^{-1} ($\nu_{as}(COO^-)$), and

[*] C. Schulz-Drost, Dr. V. Sgobba, C. Gerhards, S. Leubner, R. M. Krick Calderon, A. Ruland, Prof. Dr. D. M. Guldi
Friedrich-Alexander-Universität Erlangen-Nürnberg
Department Chemie und Pharmazie und Interdisziplinäres Zentrum für Molekulare Materialien (ICMM)
Egerlandstrasse 3, 91058 Erlangen (Germany)
Fax: (+49) 9131-852-8307
E-mail: dirk.guldi@chemie.uni-erlangen.de

[**] This work was supported financially by the Deutsche Forschungsgemeinschaft (GU 517/11-1).

Supporting information for this article is available on the WWW under http://dx.doi.org/10.1002/anie.200906891.

at 1380 cm^{-1} (δ(OH)). Not detectable are, however, the characteristic S–H vibrations at roughly 2560–2580 cm^{-1} because of the formation of the sulfur–QD bond. As a consequence of QD-pyrene formation, the OH stretch band of the carboxylic acid (3410 cm^{-1}) is transformed into the N–H stretch band within CO-NH-R at 3340 cm^{-1}. The C=O stretching and N-H bending vibrations at 1640 and 1560 cm^{-1}, respectively, are also evident.[12]

Finally, stable suspensions of QD-pyrene/SWNT were generated by simply stirring an aqueous solution of QD-pyrene—with optical density of 0.1 at 420 nm—and SWNTs under an argon atmosphere for 24 h.[13] The π–π interaction between the QD-pyrene and the SWNTs results in the formation of nanohybrids.

Valuable insights into structural features were obtained by transmission electron microscopy (TEM) and high-resolution transmission electron microscopy (HRTEM). Figure S2 in the Supporting Information corroborates that the QDs are cubic zinc-blende nanocrystallites with characteristic (220) lattice plane spacing (325–328 pm). Energy-disperse X-ray (EDX) analysis gave qualitative evidence for the dominant constituents, namely cadmium, tellurium, and sulfur. Representative TEM images of the QD-pyrene/SWNT hybrids are shown in Figure 1 and Figure S3 in the Supporting Information. Clearly, SWNT debundling is far from quantitative, as SWNT bundles with diameters ranging from 60 to 120 nm are present. Regardless of the presence of SWNT bundles, there is clear evidence that individual QD-pyrene units are immobilized on SWNTs. To rule out particulates such as catalyst nanoparticles, additional HRTEM images were recorded (see Figure S4 in the Supporting Information). Unquestionably, the monocrystallinity within the individual particles originates from QD-pyrene nanoconjugates. Moreover, an interplanar spacing of approximately 327 pm correlates with the cubic zinc-blende structure of the QDs and is consistent with the results from HRTEM investigations of pure QDs.[14] Importantly, there was no evidence for aggregated QDs.

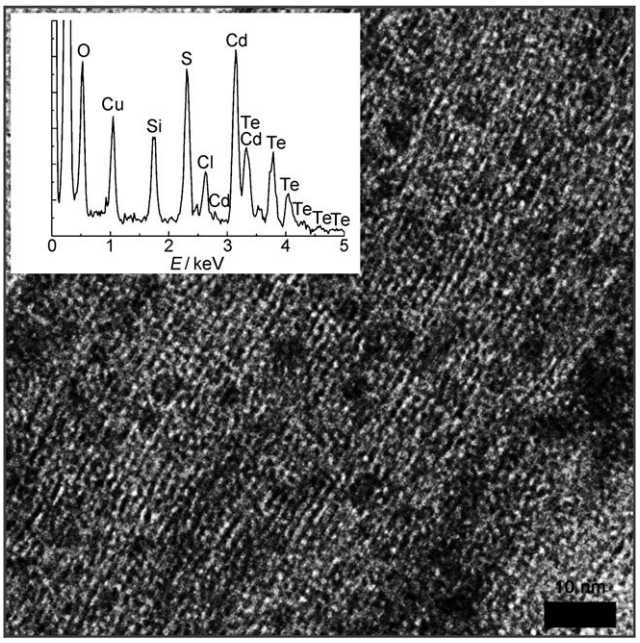

Figure 1. TEM image and EDX pattern (inset) of QD-pyrene/SWNT nanohybrids.

EDX analysis verified that the QD-pyrene nanoconjugates consist mainly of Cd, Te, S, and C (see inset in Figure 1). Since comparable data were acquired for numerous locations on the grid, we must conclude that individual QD-pyrene nanoconjugates were successfully immobilized onto uniformly distributed SWNT bundles.

Further evidence for the formation of QD-pyrene/SWNT nanohybrids came from spectroscopic investigations of pure QDs, QD-pyrene, and QD-pyrene/SWNT (Figure 2). In line

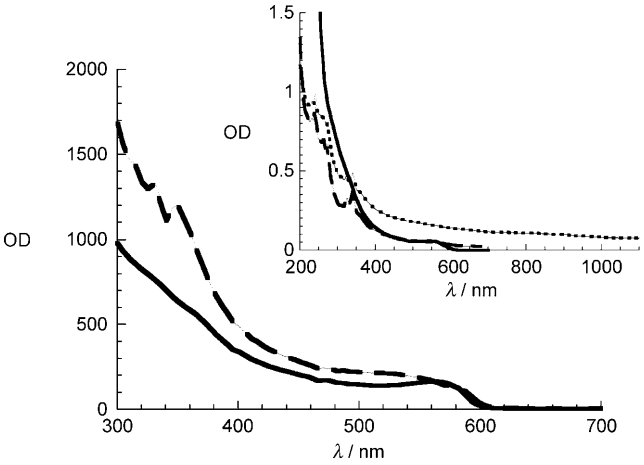

Figure 2. Excitation spectra of CdTe QDs (solid line) and QD-pyrene (dashed line) recorded at 586 and 599 nm, respectively, which correspond to luminescence maxima in aqueous solution at room temperature. Inset: Absorption spectra of CdTe QDs (solid line), QD-pyrene (dashed line), and QD-pyrene/SWNT (dotted line) in aqueous solution.

with the QDs' quantum confinement, absorption maxima, which are ascribed to the electronic transition across the band gap, are clearly visible in the 500—550 nm range. A comparison of differently sized QDs led to continuously shifting maxima. In particular, shifts to lower energies emerge as the particle size increases. This trend reflects decreasing QD band gaps. An illustration is given in the inset in Figure 2, in which the absorption features of red QDs with an absorption maximum at 544 nm are depicted.

In the absorption spectrum of QD-pyrene the signatures of the two constituents, that is, QD and 1-pyrenemethylamine, are discernable. Importantly, the typical π–*π transitions in the region between 200 and 400 nm appear unchanged in QD-pyrene and in 1-pyrenemethylamine. Coupling 1-pyrenemethylamine to QDs imposes, however, notable changes to the characteristic QD band-gap transitions. In QD-pyrene, the absorption maximum is 1) shifted bathochromically by approximately 15 nm, 2) broadened, and 3) slightly decreased in intensity (i.e., by 16%). Although QD-pyrene, like QD, can still be suspended in water, the solutions appear slightly more turbid after the coupling reaction as a result of the introduction of nonpolar 1-pyrenemethylamine onto the QD surface. Consequently, we ascribe the lower transmittance to light scattering caused by incompletely dispersed/individual QD-pyrene nanoconjugates.[15]

In the absorption spectrum of the QD-pyrene/SWNT nanohybrids (see inset in Figure 2) 1-pyrenemethylamine transitions are registered in the ultraviolet range, at 240, 275, and 340 nm. Transitions in the visible and in particular in the near-infrared range, on the other hand, correspond to suspended and sufficiently debundled SWNTs, as optical transitions between van Hove singularities become discernable. Notable, the characteristic QD band-gap absorption is superimposed onto the SWNT transitions.

All QD samples display bright band-gap luminescence. Like the absorption, the luminescence is dependent on QD size, and the color changes from green to yellow to orange to red (see Figure S5 in the Supporting Information). In the case of red QDs a symmetric luminescent maximum is seen at 586 nm with a quantum yield of 12% (Figure 3). The corresponding excitation spectra of the luminescence at 586 nm led to features that are in excellent agreement with the ground-state absorption features including a band gap onset at 610 nm (see Figure 2).

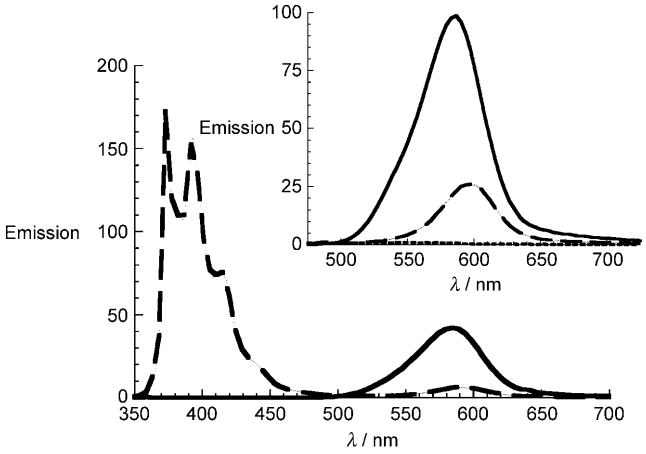

Figure 3. Luminescence and fluorescence spectra of CdTe QDs (solid line) and QD-pyrene (dashed line) in aqueous solution upon excitation at 320 nm and at room temperature. Inset: Luminescence spectra of CdTe QD (solid line), QD-pyrene (dashed line), and QD-pyrene/SWNT (dotted line) in aqueous solution upon excitation at 420 nm and at room temperature. In all of these experiments the solutions exhibit an optical density of 0.1 at the excitation wavelength.

Owing to the distinct absorptions of both QD and 1-pyrenemethylamine, we performed emission experiments with QD-pyrene with excitation at 320 nm (Figure 3) and at 420 nm (inset in Figure 3). Excitation at 320 nm is preferential for the π–π* transitions of 1-pyrenemethylamine and brings about fluorescence peaks at 373, 393, and 414 nm. The pyrene-related quantum yields in water differ drastically in 1-pyrenemethylamine and QD-pyrene with values of 41.4% [16] and 14.1%, respectively. At lower energies, that is, between 500 and 700 nm, we note the typical QD band-gap luminescence, despite excitation of the π–π* transitions that are formed quantitatively. Spectroscopic evidence for the associated deactivation mechanism, that is, a transduction of excited state energy, came from excitation spectra. Here, we followed the QD luminescence as it gives rise to features that resemble the ground-state absorption spectra of 1-pyrenemethylamine (i.e., maxima at 310, 325, and 340 nm) and of QD (i.e., band-gap onset at 610 nm; see Figure 2).

On the other hand, in the experiments with excitation at 420 nm the following characteristics evolve for QD-pyrene: 3% quantum yield (i.e., fourfold quenching relative to QD) and luminescence maximum at 599 nm (i.e., 13 nm bathochromic shift relative to QD). Since the band-gap onset remains invariable in QD and QD-pyrene we rule out changes in particle size and postulate that lower-lying surface states/traps, which are generated as a consequence of coupling 1-pyrenemethylamine to QDs, are responsible for the differences.[17]

Turning to QD-pyrene/SWNT, we notice, despite the dominating SWNT features in the range of the QD-pyrene band-gap absorption (i.e., 550 nm), the characteristic QD-associated luminescence upon excitation at 420 nm. Notable is that while the luminescence of QD-pyrene is bathochromically shifted relative to QD, in QD-pyrene/SWNT the original QD attributes are restored. The underlying blue-shift is in line with the fact that now 1-pyrenemethylamine/SWNT rather than QD/1-pyrenemethylamine couplings dominate. Most significant is, however, the nearly quantitative quenching of the band-gap luminescence (quantum yield 0.13%; Figure 3). This aforementioned description refers to a snapshot after 24 hours. For this reason, we also recorded luminescence spectra in 20 minutes intervals up to a total of 13 hours (see Figure S6 in the Supporting Information). These spectra show a continuous progression in terms of luminescence quenching and hypsochromic shifting.

As a complement to the steady-state measurements, luminescence lifetimes were gathered by time-correlated single-photon counting upon excitation at 467 nm (see Figure S7 in the Supporting Information). All of the luminescence time profiles were analyzed by multiexponential fitting functions. Specifically, for QD, the dominating decay exhibits a lifetime of 34.8 ns, followed by a minor component with 12.3 ns. Additionally, 3D time-resolved emission scans were performed to study alternative decay channels such as chemical or conformational surface modifications. However, the lack of spectral changes suggests that in QDs the lifetimes stem exclusively from excitonic recombination of electron–hole pairs (Figure S8 in the Supporting Information).

In the time-resolved emission studies for QD-pyrene, the lifetime of the major component is shortened, relative to QD, to 6.9 ns.[18] Overall, this validates our assumption that the QDs and 1-pyrenemethylamine interact electronically.[19] In QD-pyrene/SWNT—concomitant to the virtually complete luminescence quenching observed in steady-state emission experiments—a drastically shortened luminescence lifetime of 120 ps relative to QD was detected.[20]

Next, ultrafast relaxation processes in QDs were probed by means of transient absorption changes with femtosecond time resolution. Upon photoexcitation at 425 nm, the spectra reveal the instantaneous formation of a very short-lived (i.e., 0.6 ps) intermediate, whose sharp absorption displays a minimum at 497 nm. Please note that changing the excitation wavelength from 425 nm to either 470 or 387 nm resulted in a red- and blue-shift of the sharp minimum to 553 and 445 nm, respectively. A likely rationale implies that an electronic

transition across the band gap creates a "hot" excited state with excess thermal energy.[21] Once it relaxes, formation of the strongly correlated excitonic electron–hole pair proceeds rapidly (i.e., 150 fs). Spectroscopically, the differential absorption changes of the excitonic electron–hole pair in QDs are dominated by rather broad transient bleaching that spans from 480 to 625 nm with a minimum at around 560 nm (Figure 4, top). As time progresses, we notice an overall intensity decrease of the bleaching owing to the population of deep traps (i.e., 9.3 ps) and shallow traps (i.e., 53.3 ps) and a red-shift. Beyond this, the transient is stable; this was confirmed by transient absorption spectroscopy employing nanosecond laser pulses. In this context, the spectral fingerprint of the coupled electron–hole pair, which is generated immediately after the nanosecond excitation, serves as a reliable probe. In fact, its position around 580 nm coincides with the transient bleaching seen after 3 ns of the femtosecond experiments (Figure S10 in the Supporting Information). Important is the fact that the kinetics of the bleaching recovery—with a lifetime of 26 ns—resemble those seen in the time-resolved luminescence assays.

Differential absorption changes that were registered for QD-pyrene are—similar to what was seen for QD—dominated by the 497 nm signature of the intermediate. The latter is subject to a quick (i.e., 0.6 ps) relaxation to yield a strongly correlated electron–hole pair (see Figure S11 in the Supporting Information). A closer look reveals, however, some subtle changes (i.e., kinetically and spectroscopically). In stark contrast to QDs, a significant faster deactivation of the excited state with lifetimes of 5.6 and 44.8 ps as major components is deduced for QD-pyrene, and the bleaching recovery is accompanied by a strong red-shift of the transient minimum to 582 nm. In line with our observation for QD, a long-lived excited state remains absorbing at the conclusion of the femtosecond time scale, namely 3 ns. Again this required examining the electron–hole recombination dynamics on the nanosecond time scale. Here, we note a distinct bleaching at around 590 nm with a short decay lifetime of 13 ns that agrees well with the luminescence decay.

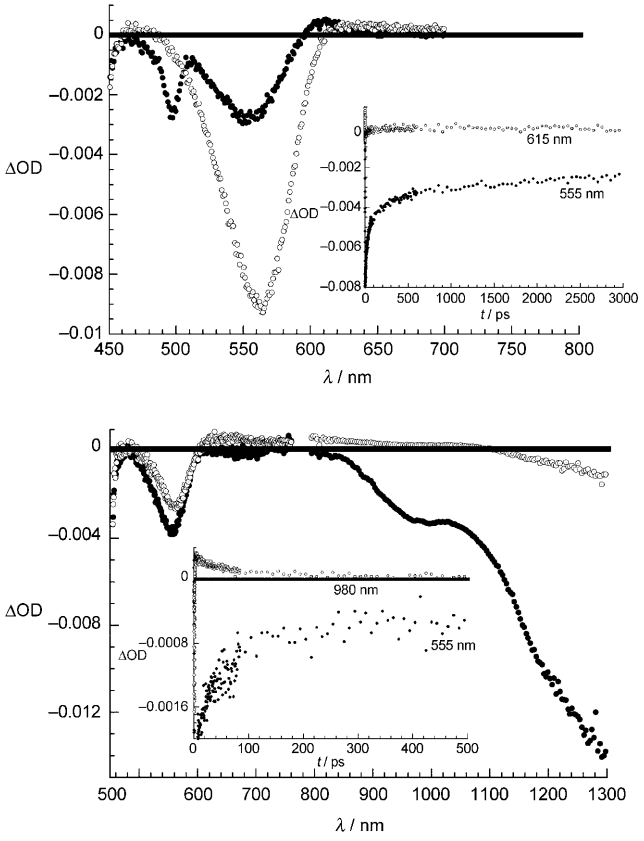

Figure 4. Differential absorption spectra from room-temperature femtosecond flash photolysis (425 nm) of pure CdTe QDs in water with time delays of 0.45 ps (●) and 1.04 ps (○) (top) and of QD-pyrene/SWNT in water with time delays of 0.72 ps (●) and 3.6 ps (○) (bottom). Inset: Time–absorption profiles of the spectra shown above; top: recorded at 555 (●) and 615 nm (○); bottom: recorded at 555 (●) and 980 nm (○).

In studies of the excited-state dynamics of QD-pyrene/SWNT, two sets of features are discernable in the corresponding transient absorption spectra following excitation at 425 nm (Figure 4, bottom). One set, which dominates in the visible range, corresponds to QD-pyrene. Here, an initially formed sharp transient with a minimum at 497 nm (i.e., higher-lying excited state) transforms into a rather broad feature with a minimum at 560 nm (i.e., excitonic electron–hole pair state). The second set of features ranges up to the near-IR. These are features that correlate with SWNT-associated excited states in the form of mirror images to the ground-state absorption—including minima at 990 and 1257 nm and a maximum at 1022 nm. In contrast to the differential absorption changes seen for QD and QD-pyrene, the transient bleaching in QD-pyrene/SWNT decays rapidly with lifetimes of 2.6 and 62 ps as major components. Importantly, the 990 and 1257 nm minima of SWNT transform within the same time window into new features (i.e., minima at 976 and 1231 nm as well as maxima at 785 and 1085 nm). From this we conclude that the 62 ps component reflects the charge-transfer reaction commencing with the QD-pyrene singlet excited state.[22] Implicit is an overall blue-shift of the SWNT-associated transitions—a feature that has been confirmed previously in spectroelectrochemical and pulse radiolytical reduction experiments[10a,23] and, in turn, has been linked to new conduction-band electrons in semiconducting SWNTs. Notable is that the charge-transfer state is metastable and decays with a lifetime of 5 ns to quantitatively regenerate the ground state.

In summary, by virtue of covalent bonds (EDC/NHS-mediated peptide condensation) and noncovalent forces (π–π interactions), water-soluble QDs and SWNTs form complexes en route to versatile donor–acceptor inorganic–organic nanohybrids, QD-pyrene/SWNT. The complementary use of spectroscopic and microscopic techniques confirmed the hierarchical integration of the electronically coupled constituents, namely QD, 1-pyrenemethylamine, and SWNT. A thorough photophysical investigation (i.e., luminescence and transient absorption measurements) sheds light on the formation of "hot" excited states, vibrational relaxation (i.e., 0.6 ps), formation of strongly correlated excitonic electron–hole pairs (i.e., 150 fs), trapping (i.e., 9.3 and 53.3 ps), and radiative recombination of excitonic electron–

hole pairs (i.e., 35 ns). The processes are summarized in Scheme 2. In QD-pyrene/SWNT a competitive pathway of charge transfer (i.e., 62 ps) transforms the excitonic state of

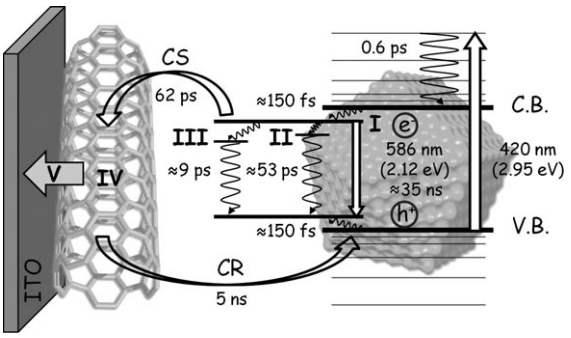

Scheme 2. Energy diagram that illustrates the deactivation pathways and related transitions with corresponding lifetimes of QD-pyrene/SWNT on ITO upon photoexcitation at 420 nm. V.B.: valence band; C.B.: conduction band; I: excitonic state of electron; II/III: surface-trapping states; IV: charge-separated state; V: electron injection into ITO; CS: charge separation; CR: charge recombination.

QD into a charge-transfer state with a lifetime of several nanoseconds. To explore the potential application of QD-pyrene/SWNT as an integrative component for the construction of photovoltaic devices, this novel nanohybrid was probed as a photoactive layer. To this end, we constructed a photoelectrochemical cell comprised of a sprayed thin film of SWNT[24] with a self-assembled[25] QD-pyrene monolayer on ITO glass as a photoelectrode, a Pt-coated FTO glass as a counter electrode, and 0.6 M 1-butyl-3-methylimidazolium iodide (BMII) and 0.3 M I_2 in methoxyacetonitrile as the electrolyte. Under AM 1.5 conditions, a short circuit current of 0.22 mA, an open circuit voltage of −0.1 V, a fill factor of 20.4%, and an efficiency of 0.0044% were measured for this setup. We believe that the current results not only document the electronic processes in solution, but sketch a potent alternative for fabricating photoactive molecular devices.

Received: December 7, 2009
Revised: March 5, 2010
Published online: June 10, 2010

Keywords: cadmium telluride · carbon nanotubes · hybrid nanostructures · quantum dots · water solubility

[1] G. D. Scholes, G. Rumbles, *Nat. Mater.* **2006**, *5*, 683.
[2] a) see Reference [7]; b) M. D. Archer, A. J. Nozik, *Nanostructured and Photoelectrochemical Systems for Solar Photon Conversion*, *Vol. 3*, Imperial College Press, London, **2006**.
[3] a) M. Stockman, *Nat. Mater.* **2004**, *3*, 423; b) S. Coe, W.-K. Woo, M. Bawendi, V. Bulovic, *Nature* **2002**, *420*, 800.
[4] a) K. Ai, B. Zhang, L. Lu, *Angew. Chem.* **2009**, *121*, 310; *Angew. Chem. Int. Ed.* **2009**, *48*, 304; b) Y. Jiang, H. Zhao, N. Zhu, Y. Lin, P. Yu, L. Mao, *Angew. Chem.* **2008**, *120*, 8729; *Angew. Chem. Int. Ed.* **2008**, *47*, 8601; c) D. R. Walt, *Nat. Mater.* **2002**, *1*, 17.
[5] a) T. Pellegrino, S. Kudera, T. Liedl, A. M. Javier, L. Manna, W. J. Parak, *Small* **2005**, *1*, 48; b) I. L. Medintz, H. T. Uyeda, E. R. Goldman, H. Mattoussi, *Nat. Mater.* **2005**, *4*, 435; c) U. Resch-Genger, M. Grabolle, S. Cavaliere-Jaricot, S. Nitschke, N. T. Roland, *Nat. Methods* **2008**, *5*, 763.
[6] A. L. Rogach, T. Franzl, T. A. Klar, J. Feldmann, N. Gaponik, V. Lesnyak, A. Shavel, A. Eychmueller, Y. P. Rakovich, J. F. Donegan, *J. Phys. Chem. C* **2007**, *111*, 14628.
[7] I. Gur, N. A. Fromer, M. L. Geier, A. P. Alivisatos, *Science* **2005**, *310*, 462.
[8] Y. Yang, L. Jing, X. Yu, D. Yan, M. Gao, *Chem. Mater.* **2007**, *19*, 4123.
[9] D. Schmid, *Nanoparticles: From Theory to Application*, Wiley-VCH, Weinheim, **2004**.
[10] a) D. M. Guldi, G. M. A. Rahman, V. Sgobba, N. A. Kotov, D. Bonifazi, M. Prato, *J. Am. Chem. Soc.* **2006**, *128*, 2315; b) L. Hu, Y. L. Zhao, K. Ryu, C. Zhou, J. F. Stoddart, G. Gruner, *Adv. Mater.* **2008**, *20*, 939; c) V. Sgobba, D. M. Guldi, *Chem. Soc. Rev.* **2009**, *38*, 165.
[11] C. Schulz-Drost, V. Sgobba, D. M. Guldi, *J. Phys. Chem. C* **2007**, *111*, 9694.
[12] a) K. Hoppe, E. Geidel, H. Weller, A. Eychmueller, *Phys. Chem. Chem. Phys.* **2002**, *4*, 1704; b) B. J. Landi, S. L. Castro, H. J. Ruf, C. M. Evans, S. G. Bailey, R. P. Raffaelle, *Sol. Energy Mater. Sol. Cells* **2005**, *87*, 733; c) R. M. Silverstein, F. X. Webster, D. Kiemle, D. J. Kiemle, *Spectrometric Identification of Organic Compounds*, 7th ed., Wiley, New York, **2005**, p. 72.
[13] Detailed information on the synthetic procedures is given in the Supporting Information.
[14] B. Tang, J. Niu, C. Yu, L. Zhuo, J. Ge, *Chem. Commun.* **2005**, 4184.
[15] All emission spectra of QD-pyrene were therefore corrected for the scattering effects.
[16] K. G. Thomas, P. V. Kamat, *J. Am. Chem. Soc.* **2000**, *122*, 2655.
[17] a) V. I. Klimov, D. W. McBranch, C. A. Leatherdale, M. G. Bawendi, *Phys. Rev. B* **1999**, *60*, 13740; b) S. Mayilo, J. Hilhorst, A. S. Susha, C. Höhl, T. Franzl, T. A. Klar, A. L. Rogach, J. Feldmann, *J. Phys. Chem. C* **2008**, *112*, 14589.
[18] The minor components gave rise to values of 30.3 and 1.6 ns.
[19] TRES measurements (Figure S9 in the Supporting Information) corroborate the lack of structural changes during the decay of the QD-pyrene excited state.
[20] The minor components for QD-pyrene/SWNT lead to values of 3.6 and 0.7 ns.
[21] a) A. J. Nozik, *Annu. Rev. Phys. Chem.* **2001**, *52*, 193; b) H. Wang, C. D. M. Donegá, A. Meijerink, M. Glasbeek, *J. Phys. Chem. B* **2006**, *110*, 733.
[22] Control experiments, in which SWNTs were exclusively excited at 778 nm, led only the deactivation of the SWNT-associated features.
[23] a) D. M. Guldi, M. Marcaccio, D. Paolucci, F. Paolucci, N. Tagmatarchis, D. Tasis, E. Vazquez, M. Prato, *Angew. Chem.* **2003**, *115*, 4338; *Angew. Chem. Int. Ed.* **2003**, *42*, 4206; b) C. Ehli, C. Oelsner, D. M. Guldi, A. Mateo-Alonso, M. Prato, C. Schmidt, C. Backes, F. Hauke, A. Hirsch, *Nat. Chem.* **2009**, *1*, 243; c) L. Kavan, L. Dunsch, *ChemPhysChem* **2007**, *8*, 974.
[24] W. Lee, J. Lee, S.-H. Lee, J. Chang, W. Yi, S.-H. Han, *J. Phys. Chem. C* **2007**, *111*, 9110.
[25] M. A. Herranz, C. Ehli, S. Campidelli, M. Gutierrez, G. L. Hug, K. Ohkubo, S. Fukuzumi, M. Prato, N. Martin, D. M. Guldi, *J. Am. Chem. Soc.* **2008**, *130*, 66.

